ISSN (Print) 1226-1750
ISSN (Online) 2233-6656
**Journal of Magnetics** 26(3), 271-276 (2021) https://doi.org/10.4283/JMAG.2021.26.3.271

# Comparative Work for Darcy-Forchheimer Hybrid Nanofluid Flow Subject to Zinc Ferrite, Nickle Zinc Ferrite

**Faris Alzahrani[1] and M. Ijaz Khan[1,2]***

[1]*Nonlinear Analysis and Applied Mathematics (NAAM)-Research Group, Department of Mathematics, Faculty of Sciences, King Abdulaziz University, P.O. Box 80203, Jeddah 21589, Saudi Arabia*
[2]*Department of Mathematics and Statistics, Riphah International University I-14, Islamabad 44000, Pakistan*

(Received 3 April 2021, Received in final form 4 July 2021, Accepted 7 July 2021)

**Owing to thermal requirements of many industrial and engineering processes, this research presents the improved feature of hybrid nanofluid with applications heat source and sinks features. The most fascinating Zinc ferrite and Nickle Zinc ferrite nanoparticles are used to predict the thermal enhancement in engine oil and Kerosene oil base materials. The radiative phenomenon with nonlinear relations is encountered to enhance the heat transportation pattern. Moreover, the entropy generation assessment is also observed with significances of optimized analysis. The consideration of porous space is inspected by using the Darcy-Forchheimer theory. A comprehensive comparative analysis for enchantment of heat transfer rate is examined between both types of nanoparticles. The physical influence of parameters for velocity, thermal gradient and entropy generation phenomenon is visualized. It is observed that thermal efficiency of ferrite nanoparticles ($MnZnFe_2O_4$) with suspension of engine oil ($C_8H_{18}$) base liquid is more progressive as compared to the suspensions of ferrite nanoparticles and kerosene oil ($C_{10}H_{22}$) hybrid material.**

**Keywords :** hybrid nanofluid, darcy-forchheimer flow, slip effects, entropy generation

## 1. Introduction

The ongoing revulsion in the nano-technology and thermal engineering, the scientists have successfully found out the new impressive source of energy with interaction of modern nanoparticles. The declined thermal availability of base liquids always pronounced a lower thermal energy effusion and subsequently reduces the industrial and engineering products. The nanoparticles with millimetre size are preferred to improve the conventional base particles thermal efficiency. The advancement in the thermal engineering also claimed the use of nanoparticles as a coolant. The enhancement in heat transfer characteristics is observed due to proper utilization of nanoparticles. The improved thermal mechanism of nano-materials reflects valuable attention in the transportation systems, extrusion processes, nuclear reactions, bio-medical applications etc. The motivating idea behind the improvement of thermal efficiency is owing to the justification that the thermal conductivity of suspended metallic particles is higher as compared to the base liquids like ethylene and water. The length of such nanoparticles is usually claimed as 1-100 nm. Choi [1] pointed out the basic research on this topic and experimentally explored the thermal prospective of nanoparticles. This novel investigation insisted many researchers to work and explore more thermal insight of nanoparticles. Majee and Shit [2] addressed the magnetized nanoparticles thermal inspection regarding the blood flow in stenosed artery with support of numerical computations. Waqas *et al.* [3] identified the bio-convective prospective for nanofluids with generalized viscoelastic fluid. Khan [4] pointed out the hybrid nanoparticles useful thermal inspection for the rotating disk flow in porous space via Darcy-Forchheimer theory. The shape and size of nanoparticles containing the gold and silver particles under the novel influence of multiple slip was visualized by Mathew *et al.* [5]. Hussain *et al.* [6] focused on the instability measurements of oxide nanoparticles immersed with water. The thermophysical aspects in hybrid nanofluid consists of AA7072-AA7075 nanoparticles attended by curved geometry was computed in the investigation of Madhukesh *et al.* [7]. Khan and Alzahrani [8] performed


*Corresponding author: Tel: +92-300-9019713
Fax: +92-300-9019713, e-mail: mikhan@math.qau.edu.pk

thermal assessment for Jeffrey nanofluid under optimized constraints accounted by curved stretched configuration. Qasemand Mdallal [9] pointed out the improvement in heat transmissions due to $Al_2O_3$ and silicon suspension due to disk which rotates uniformly. Rashid *et al.* [10] characterized the enhanced prospective of heat pattern due to $TiO_2$ and Ag nanoparticles additionally explaining the shape consequences over cylinder. The velocity slip enrolment for radiative flow of silicon dioxide nanoparticles has been identified by Khan and Alzahrani [11].

The thermodynamics optimization associated to many industrial and engineering phenomenons has engaged the main contributions to enhance the effectiveness and sustainability of thermal processes. The modifications in the thermal systems and heat transportation mechanisms are done by following the theory of thermodynamics. The first law of thermodynamics guaranteed the transformation of energy between various systems is observed without loss of energy. It is critically observed that the optimized analysis (irreversibilities) is not justified on the basis of this theory. The directions of second law of thermodynamics reveal the consumptions of energy and control the energy loss which compiled the enhancements of thermal efficiency in heating transportation systems. Bejan [12] contributed the pioneer work on entropy generation analysis for inspecting the heat transfer pattern. Kumar *et al.* [13] discussed the convective heat analysis with entropy generation consideration numerically. Alsaedi *et al.* [14] described the optimized analysis for Williamson nanofluid with improved activation energy features. Aghakhani *et al.* [15] evaluated the role of elliptic constant temperature gradient for the entropy generation flow of alumina nanoparticles. Shukla *et al.* [16] discussed the optimized consequences regarding the non-Newtonian flow. The prediction of entropy generation with reactive species for viscoelastic materials has been directed in the contribution of Khan *et al.* [17]. Salimi *et al.* [18] evaluated the pattern of entropy analysis in porous jet with convective heat transfer transport. Seyyedi *et al.* [19] inspected the change in heat transfer regarding the optimized flow in enclosure with implementation of magnetic force.

Motivating with the inspired applications of nanoparticles and optimized phenomenon, this research predicts the thermal significances of hybrid nanofluid containing the manganese Zinc ferrite ($MnZnFe_2O_4$) and Nickle Zinc ferrite ($NiZnFe_2O_4$) nanoparticles in presence of Kerosene oil and engine oil. The novel motivations of this analysis are to presents a comparative analysis for the thermal improvement of Kerosene oil and engine oil properties by utilizing the two types of nanoparticles. Moreover, the entropy generation phenomenon is also performed to control the heat transfer rate and loss in energy. A clear comparative analysis is highlighted with change in thermal performances of base fluids. This analysis directs useful directions to enhance the thermal efficiency of engine oil associated to the applications of vehicles and mechanical devices.

## 2. Mathematical Formulation

Here two-dimensional, steady Darcy-Forchheimer flow of an incompressible hybrid nanoliquid is addressed. Slip effect is considered at boundary. Heat analysis is discussed through first law of thermodynamics. Physical description of irreversibility is accounted. Here manganese Zinc ferrite and Nickle Zinc ferrite are used as nanoparticles. While engine oil and Kerosene oil are used as basefluids. We consider $u_w = ax$ as stretching velocity with rate constant ($a > 0$).

The governing expression satisfy:

$$\frac{\partial u}{\partial x}+\frac{\partial v}{\partial y}=0, \tag{1}$$

$$\left(u\frac{\partial u}{\partial x}+v\frac{\partial u}{\partial y}\right)=\nu_{hnf}\frac{\partial^2 u}{\partial y^2}-Fu^2-\frac{\nu_{hnf}}{K^*}u, \tag{2}$$

$$\left(u\frac{\partial T}{\partial x}+v\frac{\partial T}{\partial y}\right)=\frac{k_{hnf}}{(\rho C_p)_{hnf}}\frac{\partial^2 T}{\partial y^2}, \tag{3}$$

The boundary conditions for the above prescribed model are:

$$u=ax+\lambda_1\frac{\partial u}{\partial y},\ v=0,\ T=T_w \ \text{at}\ y=0$$
$$u\to 0,\ T\to T_\infty \ \text{at}\ y\to\infty \tag{4}$$

In above expression ($u$, $v$) characterize the velocity components, $K^*$ the porous medium permeability, $\rho_{hnf}$ the density, $\mu_{hnf}$ the viscosity, $T$ the temperature, ($x$, $y$) the Cartesian coordinates, $c_p$ the specific heat, $T_w$ the surface temperature, $\lambda_1$ the slip coefficient, $k_{hnf}$ the thermal conductivity, $T_\infty$ the ambient temperature, $F=\frac{c_b}{x\sqrt{K^*}}$ the

**Table 1.** Thermo physical properties of base fluid and ferrite nanoparticles.

| Physical properties | P ($kg/m^3$) | $C_p$ (J/kgK) | $k$ (W/mK) | Pr |
|---|---|---|---|---|
| $C_8H_{18}$ | 890 | 1868 | 0.145 | 12900 |
| $C_{10}H_{22}$ | 783 | 2090 | 0.15 | 21 |
| $MnZnFe_2O_4$ | 4700 | 1050 | 3.9 | - |
| $NiZnFe_2O_4$ | 4800 | 710 | 6.3 | - |

Forchheimer number coefficient, $(\rho Cp)_{hnf}$ the heat capacitance of hybrid nanofluid.

Thermophysical properties for different combinations are mentioned in Tables 1-3.

Considering

$$\xi = y\sqrt{\frac{a}{\nu_f}},\ u = axf'(\xi),\ v = -\sqrt{a\nu_f}\,f(\xi),\ \theta(\xi) = \frac{T-T_\infty}{T_w-T_\infty} \quad (5)$$

Dimensionless version are

$$\frac{f'''}{(1-\phi_1)^{5/2}(1-\phi_2)^{5/2}A_1} + ff'' - f'^2 - F_r f'^2 - \frac{\beta}{(1-\phi_1)^{5/2}(1-\phi_2)^{5/2}A_1}f' = 0 \quad (6)$$

$$\frac{1}{\Pr A_2}\frac{k_{hnf}}{k_f}\theta'' + f\theta' = 0 \quad (7)$$

with

$$f'(0) = 1 + L_1 f''(0),\ f(0) = 0,\ \theta(0) = 1$$
$$f'(\infty) \to \theta(\infty) \to 0 \quad (8)$$

Here $\beta = \frac{\nu_f}{k^* a}$ signify the porosity parameter, $L_1 = \lambda_1\sqrt{\frac{a}{\nu}}$ the slip parameter, $Pr = \frac{(\rho C_p)_f \nu_f}{k_{f1}+k_{f2}}$ the Prandtl number, $F_r = \frac{c_b}{x\sqrt{K^*}}$ the Forchheimer parameter and $A_1$ and $A_2$ are

**Table 2.** Thermo physical properties of $MnZnFe_2O_4$-$NiZnFe_2O_4$-$C_{10}H_{22}$ and $MnZnFe_2O_4$-$NiZnFe_2O_4$-$C_8H_{18}$.

| Properties | $MnZnFe_2O_4$-$NiZnFe_2O_4$-$C_{10}H_{22}$ | $MnZnFe_2O_4$-$NiZnFe_2O_4$-$C_8H_{18}$ |
|---|---|---|
| Density ($\rho$) | $\frac{\rho_{hnf}}{\rho_f} = (1-\phi_2)\left[(1-\phi_1) + \phi_1\frac{\rho_{s1}}{\rho_f}\right] + \phi_2\frac{\rho_{s2}}{\rho_f}$ | $\frac{\rho_{hnf}}{\rho_f} = (1-\phi_2)\left[(1-\phi_1) + \phi_1\frac{\rho_{s1}}{\rho_f}\right] + \phi_2\frac{\rho_{s2}}{\rho_f}$ |
| Heat capacity ($\rho C_p$) | $\frac{(\rho Cp)_{hnf}}{(C_p\rho)_f} = (1-\phi_2)\left[(1-\phi_1) + \phi_1\frac{(\rho Cp)_{s1}}{(\rho C_p)_f}\right] + \phi_2\frac{(\rho Cp)_{s2}}{(\rho C_p)_f}$, | $\frac{(\rho Cp)_{hnf}}{(C_p\rho)_f} = (1-\phi_2)\left[(1-\phi_1) + \phi_1\frac{(\rho Cp)_{s1}}{(\rho C_p)_f}\right] + \phi_2\frac{(\rho Cp)_{s2}}{(\rho C_p)_f}$ |
| Viscosity ($\mu$) | $\mu_{hnf} = \frac{\mu_f}{(1-\phi_1)^{2.5}(1-\phi_2)^{2.5}}$ | $\mu_{hnf} = \frac{\mu_f}{(1-\phi_1)^{2.5}(1-\phi_2)^{2.5}}$ |
| Thermal conductivity | $\frac{k_{hnf}}{k_{bf}} = \frac{k_{s2}+2k_{bf}-2\phi_2(k_{bf}-k_{s2})}{k_{s2}+2k_{bf}+\phi_2(k_{bf}-k_{s2})}$, $\frac{k_{bf}}{k_f} = \frac{k_{s1}+2k_f-2\phi_1(k_f-k_{s1})}{k_{s1}+2k_f+\phi_1(k_f-k_{s1})}$, | $\frac{k_{hnf}}{k_{bf}} = \frac{k_{s2}+2k_{bf}-2\phi_2(k_{bf}-k_{s2})}{k_{s2}+2k_{bf}+\phi_2(k_{bf}-k_{s2})}$, $\frac{k_{bf}}{k_f} = \frac{k_{s1}+2k_f-2\phi_1(k_f-k_{s1})}{k_{s1}+2k_f+\phi_1(k_f-k_{s1})}$ |
| Prandtl number | 21 | 12900 |

**Table 3.** Thermo physical properties of $MnZnFe_2O_4$-$NiZnFe_2O_4$-$C_{10}H_{22}$-$C_8H_{18}$.

| Properties | $MnZnFe_2O_4$-$NiZnFe_2O_4$-$C_{10}H_{22}$-$C_8H_{18}$ |
|---|---|
| $\rho$ (Density) | $\frac{\rho_{hnf}}{(\rho_{f1}+\rho_{f2})} = (1-\phi_2)\left[(1-\phi_1) + \phi_1\frac{(\rho_{s1}+\rho_{s2})}{(\rho_{f1}+\rho_{f2})}\right] + \phi_2\frac{(\rho_{s1}+\rho_{s2})}{(\rho_{f1}+\rho_{f2})}$ |
| Heat capacity ($\rho C_p$) | $\frac{(\rho Cp)_{hnf}}{(\rho C_p)_{f1}+(\rho C_p)_{f2}} = (1-\phi_2)\left[(1-\phi_1) + \phi_1\left(\frac{(\rho Cp)_{s1}+(\rho Cp)_{s2}}{(\rho Cp)_{f1}+(\rho Cp)_{f2}}\right)\right] + \phi_2\frac{(\rho Cp)_{s1}+(\rho Cp)_{s2}}{(\rho Cp)_{f1}+(\rho Cp)_{f2}}$, |
| Viscosity ($\mu$) | $\mu_{hnf} = \frac{\mu_{f1}+\mu_{f2}}{(1-\phi_1)^{2.5}(1-\phi_2)^{2.5}}$ |
| Thermal conductivity | $\frac{k_{hnf}}{(k_{bf1}+k_{bf1})} = \frac{(k_{s1}+k_{s2})+2(k_{bf1}+k_{bf1})-2\phi_2((k_{bf1}+k_{bf1})-(k_{s1}+k_{s2}))}{(k_{s1}+k_{s2})+2(k_{bf1}+k_{bf1})+\phi_2(k_{bf}-(k_{s1}+k_{s2}))}$, $\frac{(k_{bf1}+k_{bf1})}{(k_{f1}+k_{f1})} = \frac{(k_{s1}+k_{s2})+2(k_{f1}+k_{f1})-2\phi_1((k_{f1}+k_{f1})-(k_{s1}+k_{s2}))}{(k_{s1}+k_{s2})+2(k_{f1}+k_{f1})+\phi_1((k_{f1}+k_{f1})-(k_{s1}+k_{s2}))}$, |
| Prandtl number | 12921 |

expressed as

$$A_1 = (1-\phi_2)\left[(1-\phi_1) + \phi_1\left(\frac{\rho_{s1}+\rho_{s2}}{\rho_{f1}+\rho_{f2}}\right) + \phi_2\left(\frac{\rho_{s1}+\rho_{s2}}{\rho_{f1}+\rho_{f2}}\right)\right]$$

$$A_2 = (1-\phi_2)\left[(1-\phi_1) + \phi_1\left(\frac{(\rho C_p)_{s1}+(\rho C_p)_{s2}}{(\rho C_p)_{f1}+(\rho C_p)_{f2}}\right) + \phi_2\left(\frac{(\rho C_p)_{s1}+(\rho C_p)_{s2}}{(\rho C_p)_{f1}+(\rho C_p)_{f2}}\right)\right]$$

## 3. Entropy Generation

Entropy generation rate can be defined as

$$S_G = \left(\frac{k_{hnf}}{k_{f1}+k_{f2}}\right)\frac{k_{f1}+k_{f2}}{T_\infty^2}\left(\frac{\partial T}{\partial y}\right)^2 + \frac{\mu_{hnf}}{T_\infty}\left(\frac{\partial u}{\partial y}\right)^2 + \frac{\mu_{hnf}}{k^* T_\infty}u^2 \tag{9}$$

$$N_G = \alpha_1\left(\frac{k_{hnf}}{k_{f1}+k_{f2}}\right)(\theta')^2 + \frac{Br}{(1-\phi_1)^{2.5}(1-\phi_2)^{2.5}}(f'')^2 + \frac{Br\beta}{(1-\phi_1)^{2.5}(1-\phi_2)^{2.5}}(f')^2 \tag{10}$$

In above expression $N_G = \frac{S_G T_\infty \nu}{k\Delta T a}$ denotes the entropy number, $\alpha_1 = \frac{T_w - T_\infty}{T_\infty}$ the temperature difference variable and $Br = \frac{\mu_f (ax)^2}{(k_{f1}+k_{f2})\Delta T}$ the Brinkman number.

## 4. Physical Quantities

The physical quantities of interest (gradient of velocity and heat transfer rate) are given as

$$C_{fx} = \frac{\tau_w}{\rho_f (u_w)^2},\ Nu_x = \frac{x q_w}{k_f (T_w - T_\infty)} \tag{11}$$

Whereshear stresses ($\tau_w$) andheat flux ($q_w$) are defined as

$$\tau_w = \mu_{hnf} w\left(\frac{\partial u}{\partial y}\right),\ q_w = -k_{hnf}\left(\frac{\partial T}{\partial y}\right) \tag{12}$$

We have

$$C_{fx}\,\mathrm{Re}_x^{1/2} = \frac{1}{(1-\phi_1)^{2.5}(1-\phi_2)^{2.5}} f''(0),\ Nu_x\,\mathrm{Re}_x^{-1/2} = -\frac{k_{hnf}}{k_f}\theta'(0) \tag{13}$$

## 5. Results and Discussion

The obtained system is solved numerically and investigated with the support of graphs. Physical description of velocity, entropy generation number, temperature and Bejan number versus various flow variables are discussed through graphs. Computational outcomes of drag force and heat transfer rate for different types of nanoparticles against pertinent variables are highlighted through Table 4. Here all these investigation for three different kind of solution $MnZnFe_2O_4$-$NiZnFe_2O_4$-$C_{10}H_{22}$-$C_8H_{18}$, $MnZnFe_2O_4$-$NiZnFe_2O_4$-$C_{10}H_{22}$ and $MnZnFe_2O_4$-$NiZnFe_2O_4$-$C_8H_{18}$.

### 5.1. Velocity distribution

Influence of various sundry parameters on velocity field by considering three different kind of solution $MnZnFe_2O_4$-$NiZnFe_2O_4$-$C_{10}H_{22}$-$C_8H_{18}$, $MnZnFe_2O_4$-$NiZnFe_2O_4$-$C_{10}H_{22}$ and $MnZnFe_2O_4$-$NiZnFe_2O_4$-$C_8H_{18}$ are exhibited in Figs. 1-7. Variation of Forchheimer number on velocity for two different type of solutions is illuminated in Fig. 1. One can find that velocity profile of the ferrite nanoparticles suspended in hybrid base liquid reduces faster than ferrite nanoparticles suspended in Kerosene and engine oils. Figs. 2, 3 sketch to demonstrate the influence of $\phi_1$ and $\phi_2$ on velocity profile for two different kinds of solution. An increment in volume fraction ($\phi_1$ and $\phi_2$) corresponds to diminishes velocity profile. One can find that faster reduction occurs in fluid motion for ferrite nanoparticles

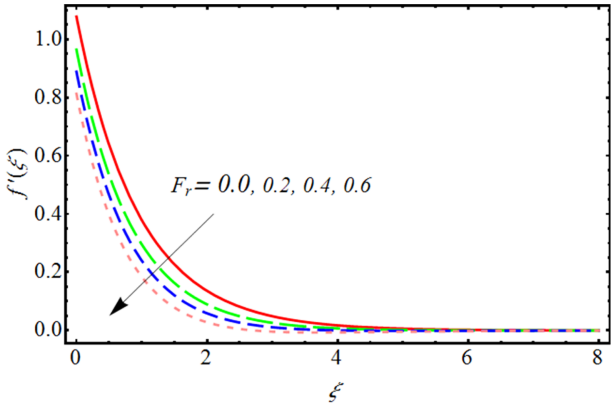


**Fig. 1.** (Color online) Impact of Darcy-Forchheimer parameter on velocity.

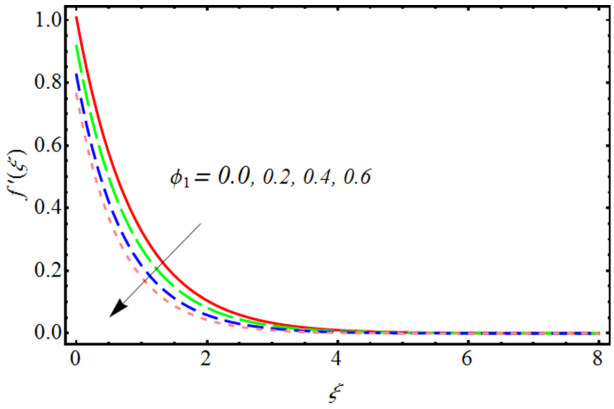


**Fig. 2.** (Color online) Impact of $\phi_1$ on velocity.

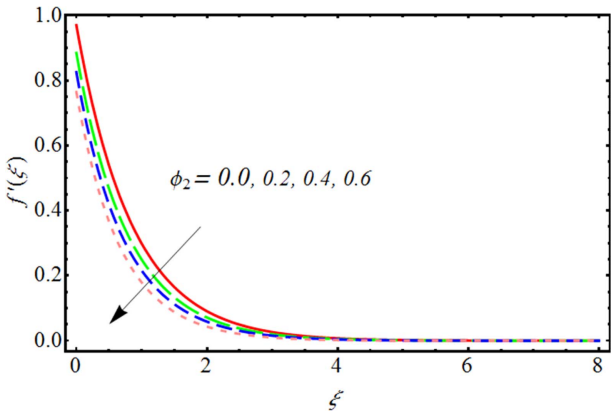


**Fig. 3.** (Color online) Impact of $\phi_2$ on velocity.

($MnZnFe_2O_4$-$NiZnFe_2O_4$) delimited in hybrid base fluid $C_{10}H_{22}$-$C_8H_{18}$ when compared to other solutions.

### 5.2. Thermal field

Salient features of volume fraction ($\phi_1$ and $\phi_2$) on thermal field for two different kind of solution is scrutinized in Figs. 4, 5. An improvement occurs in thermal field with the variation in volume fraction ($\phi_1$ and $\phi_2$). Clearly observed that ferrite nanoparticles suspended in base liquid reduces faster than ferrite nanoparticles suspended in hybrid base liquid.

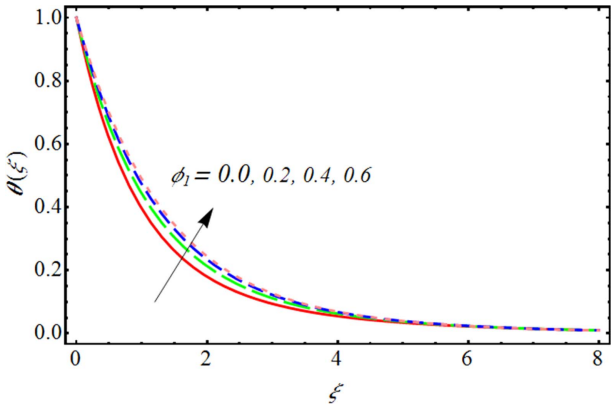


**Fig. 4.** (Color online) Impact of $\phi_1$ on temperature.

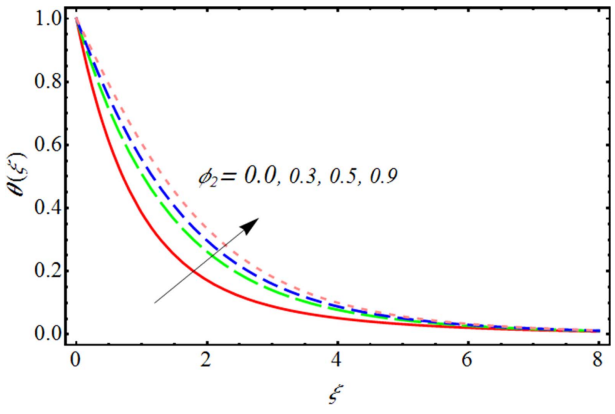


**Fig. 5.** (Color online) Impact of $\phi_2$ on temperature.

### 5.3. Influence of various parameters on Entropy generation and Bejan number

Figs. 6, 7 are depicted to examine the characteristics features of entropy generation and Bejan number for considering three different solutions namely $MnZnFe_2O_4$-$NiZnFe_2O_4$-$C_{10}H_{22}$-$C_8H_{18}$, $MnZnFe_2O_4$-$NiZnFe_2O_4$-$C_{10}H_{22}$, $MnZnFe_2O_4$-$NiZnFe_2O_4$-$C_8H_{18}$. Here clearly noted from these Figs. That entropy and Bejan numbers are higher for $MnZnFe_2O_4$-$NiZnFe_2O_4$-$C_8H_{18}$ when compared to $MnZnFe_2O_4$-$NiZnFe_2O_4$-$C_{10}H_{22}$-$C_8H_{18}$ and $MnZnFe_2O_4$-$NiZnFe_2O_4$-$C_{10}H_{22}$. Impact of Brinkman number on Entropy generation is portrayed in Fig. 6. An amplification in entropy rate is noted through Brinkman number. Clearly seen that entropy number is higher for $MnZnFe_2O_4$-$NiZnFe_2O_4$-$C_8H_{18}$ as compared to $MnZnFe_2O_4$-$NiZnFe_2O_4$-$C_{10}H_{22}$-$C_8H_{18}$. Fig. 7 is depicted to show the influence of Bejan number against Brinkman number. An intensification in Brinkman number reduces the Bejan number.

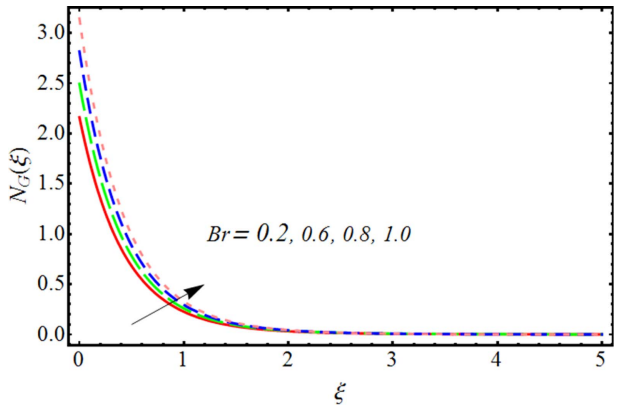


**Fig. 6.** (Color online) Impact of Br on entropy generation.

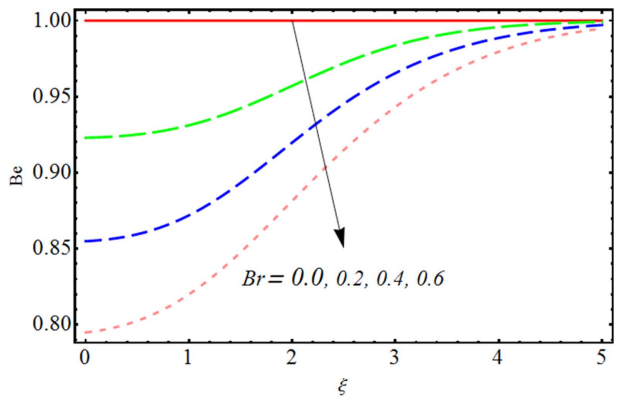


**Fig. 7.** (Color online) Impact of Br on Bejan number.

**Table 4.** Numerical values of physical quantities (drag force and Nusselt number).

| $\phi_1$ | $\phi_2$ | $C_{fx}$ | $Nu_s$ |
|---|---|---|---|
| 0.0 | 0.01 | 1.65478 | 1.12547 |
| 0.05 | | 1.43564 | 1.36542 |
| 0.1 | | 1.32546 | 1.56421 |
| 0.3 | 0.02 | 1.24563 | 1.19365 |
| | 0.05 | 1.15423 | 1.11236 |
| | 0.08 | 1.09456 | 1.056421 |

Here one can found that rate of declination is higher in $MnZnFe_2O_4$-$NiZnFe_2O_4$-$C_{10}H_{22}$-$C_8H_{18}$ compared to $MnZnFe_2O_4$-$NiZnFe_2O_4$-$C_8H_{18}$.

### 5.4. Engineering quantities

Influence of pertinent variable on physical quantities (drag force and Nusselt number) for ferrite nanoparticles subtended in hybrid base fluid $C_{10}H_{22}$-$C_8H_{18}$ is demonstrated in Table 4. From these table we observed that larger approximation of volume fraction ($\phi_1$ and $\phi_2$) leads to decays the drag force for ferrite nanoparticles suspended in hybrid base fluid $C_{10}H_{22}$-$C_8H_{18}$. While opposite is noticed for heat transfer rate.

### 5.5. Final Remarks

Motivating with the inspired applications of nanoparticles and optimized phenomenon, this research predicts the thermal significances of hybrid nanofluid containing the manganese Zinc ferrite ($MnZnFe_2O_4$) and Nickle Zinc ferrite ($NiZnFe_2O_4$) nanoparticles in presence of Kerosene oil and engine oil. The novel motivations of this analysis are to presents a comparative analysis for the thermal improvement of Kerosene oil and engine oil properties by utilizing the two types of nanoparticles. Moreover, the entropy generation phenomenon is also performed to control the heat transfer rate and loss in energy. Some significant observations for the considered examination can be gathered as:

$MnZnFe_2O_4$-$NiZnFe_2O_4$-$C_{10}H_{22}$-$C_8H_{18}$ as lower velocity when compared to other two.

- Ferrite nanoparticles subtended in hybrid-based fluid ($C_{10}H_{22}$-$C_8H_{18}$) as lower thermal gradient and nanoparticles subtended in $C_8H_{18}$ base fluid as higher thermal gradient.
- The presence of the surface slipperiness affects temperature gradient, the enhance in values of slip parameter increases the thermal gradient.
- The entropy generation and Bejan number is high in $MnZnFe_2O_4$-$NiZnFe_2O_4$-$C_8H_{18}$ when compared to $MnZnFe_2O_4$-$NiZnFe_2O_4$-$C_{10}H_{22}$-$C_8H_{18}$ and $MnZnFe_2O_4$-$NiZnFe_2O_4$-$C_{10}H_{22}$.
- $MnZnFe_2O_4$-$NiZnFe_2O_4$-$C_8H_{18}$ and $MnZnFe_2O_4$-$NiZnFe_2O_4$-$C_{10}H_{22}$ have high entropy when compared to $MnZnFe_2O_4$-$NiZnFe_2O_4$-$C_{10}H_{22}$-$C_8H_{18}$.

## References


[1] Choi, S.U.S. **231**, 99 (1995).
[2] Sreeparna Majee and G. C. Shit, European Journal of Mechanics-B/Fluids **83**, 42 (2020).
[3] H. Waqas, Sami Ullah Khan, M. Hassan, M. M. Bhatti, and M. Imran, Journal of Molecular Liquids **291**, 111231 (2019).
[4] M. Ijaz Khan, International Communications in Heat and Mass Transfer **122**, 105177 (2021).
[5] Alphonsa Mathew, Sujesh Areekara, A. S. Sabu, and S. Saleem, Surfaces and Interfaces **25**, 101267 (2021).
[6] Zakir Hussain, Asadur Rehman, Ahson Jabbar Shaikh, Kai-XinHu, Mehboob Ali, Faisal Sultan, Muhammad Shahzad, and Mohamed Altanji, Case Studies in Thermal Engineering **26**, 100998 (2021).
[7] J. K. Madhukesh, R. Naveen Kumar, R. J. Punith Gowda, B. C. Prasannakumara, G. K. Ramesh, Sami Ullah Khan, and Yu-Ming Chu, Journal of Molecular Liquids **335**, 116103 (2021).
[8] M. Ijaz Khan and Faris Alzahrani, Mathematics and Computers in Simulation **185**, 47 (2021).
[9] S. Saranya Qasem M. Al-Mdallal, Case Studies in Thermal Engineering **25**, 100943 (2021).
[10] Umair Rashid, Haiyi Liang, Hijaz Ahmad, Muhammad Abbas, Azhar Iqbal, and Y. S. Hamed, Results in Physics **21**, 103812 (2021).
[11] M. Ijaz Khan and Faris Alzahrani, International Journal of Hydrogen Energy **46**, 1362 (2021).
[12] A. Bejan, J. Heat Transf. **101**, 718 (1979).
[13] Mahesh Kumar, G. Janardhana Reddy, G. Ravi Kiran, M. A. Mohammed Aslam, and O. Anwar Beg, Heat Transfer–Asian Res. (2019) pp 1-26.
[14] Alsaadi, F. E., Hayat, T., Khan, M. I., and Alsaadi, F. E., Comput. Meth. Prog. Biomed. **183**, 105051 (2020).
[15] Saeed Aghakhani, Ahmad Hajatzadeh Pordanjani, Masoud Afrand, and Mohsen Sharifpur, Josua PMeyer, International Journal of Mechanical Sciences **174**, 105470 (2020).
[16] Nisha Shukla, Puneet Rana, and O. Anwar Bég, Nonlinear Engineering **8**, 630 (2019).
[17] Mair Khan, Amna Shahid, M. El Shafey, T. Salahuddin, and Farzana Khan, Computer Methods and Programs in Biomedicine **187**, 105246 (2020).
[18] Mohammad Reza Salimi, Mohammad Taeibi-Rahni, and Hadi Rostamzadeh, International Journal of Thermal Sciences **153**, 106348 (2020).
[19] Seyyed Masoud Seyyedi, A. S. Dogonchi, M. Hashemi Tilehnoee, M. Waqas, and D. D. Ganji, Applied Thermal Engineering **168**, 114789 (2020).